Chaotic Modeling and Simulation (CMSIM) 3: 167–178, 2021

Vibrational Resonance in Two-Dimensional Nonlinear Maps

B. Bhuvaneswari[1], S. Valli Priyatharsini[1], V. Chinnathambi[1] and S. Rajasekar[2]

[1] Department of Physics, Sadakathullah Appa College, Tirunelveli-627 011, Tamil Nadu, India.(Affiliated to Manonmaniam Sundaranar University, Tirunelveli-627012, Tamil Nadu, India)
(E-mail: thambi1959@rediffmail.com)

[2] School of Physics, Bharathidasan University, Tiruchirapalli-620 024, Tamil Nadu, India.

Abstract. In this paper, we consider two different two-dimensional nonlinear maps like Burgers map and Predator-Prey model map driven by a biharmonic signal. The biharmonic signal consists of two signals of widely different frequencies ω and Ω with $\Omega >> \omega$. These maps are interest because they appear in different physical concepts and they are produced a much richer set of dynamic patterns than those observed in continuous one. In both maps, VR occurs at the low-frequency (ω) of the biharmonic signal as the amplitude (g) and frequency (Ω) of the high-frequency signal is varied. We show the enhanced response amplitude at the low-frequency ω showing the resonance peak and hysteresis phenomenon on the response amplitude curve due to the biharmonic signal. We characterize the periodic and chaotic orbits, hysteresis and VR phenomena using bifurcation diagram, phase portrait and response amplitude

1 Introduction

The phenomenon of Vibrational Resonance (VR) in which the response of the system to a weak periodic signal can be enhanced by the application of the high-frequency periodic perturbation of appropriate amplitude. The analysis of VR has received a considerable interest in recent years after the seminal paper by Landa and McClintock [1]. The occurrence of VR has been studied in monostable [2], bistable [1,3–5], multi-stable [6–8], time-delayed systems [9–11], ground water-dependent eco system [12], coupled systems [13,14], two-level quantum system [15], nano-electromechanical resonator [16] and discrete dynamical systems [17,18]. Experimental evidence of VR in a bistable cavity surface emitting laser system [8,19,20] and in a electronic circuit [21,22] has also been studied.

So far, most of the previous work of VR has been studied in continuous-time dynamical systems described by ordinary differential equations and less work in

Received: 7 May 2021 / Accepted: 18 July 2021
 ISSN 2241-0503

discrete dynamical systems. In this, we want to analyze the occurrence of VR in certain two-dimensional discrete dynamical systems. In the present work, we numerically investigate the occurrence of VR in two different two-dimensional maps such as Burgers map and Predator-Prey model map. Usually the discrete-time systems modelled by nonlinear difference equations are more beneficial and reliable than continuous-time differential equations. It also provides efficient computational results for numerical simulations and provides rich dynamics such as stability, bifurcation and chaos phenomena as compared to continuous one.

This paper deals with the study of the occurrence of VR of two different two-dimensional maps such as Burgers map and Predator-Prey map. This paper is organized as follows. In section 2, we present the difference equations and their equilibrium points of two maps. In section 3, we numerically investigate the occurrence of VR in Burgers map and for Predator-Prey model map in section 4. Finally we summarize the results in section 5.

2 Difference Equations and Their Equilibrium Points of the maps

In this section we present the difference equations and their equilibrium points of Burgers map and Predator-Prey model map.

(i) Burgers Map:

The difference equations of Burgers map is given by

$$x_{n+1} = (1-\nu)x_n - y_n^2 = f(x_n, y_n)\ , \tag{1}$$
$$y_{n+1} = (1+\mu)y_n + x_n y_n = g(x_n, y_n)\ , \tag{2}$$

where ν and μ are the parameters. This pair of coupled difference equations used by Burgers [23] to illustrate the relevance of the concept of bifurcations to the study of hydrodynamical flows. Recently, ELabbasy et al. [24] studied the bifurcation analysis, chaos and control in the Burgers mapping and Senkerik et al. [25] analyzed the evolutionary control of chaotic Burgers Map by means of chaos enhanced differential evolution. The map has three fixed points such as $(i)E_0 = (x^*, y^*) = (0,0), (ii)E_1 = (x^*, y^*) = (-\mu, \sqrt{\mu\nu})$ and $(iii)E_2 = (x^*, y^*) = (-\mu, -\sqrt{\mu\nu})$). Where E_1 and E_2 are symmetric fixed points. The stability determining eigenvalues are obtained from the following determinant,

$$\det(M - \lambda I) = \begin{vmatrix} 1-\nu-\lambda & -2y^* \\ y^* & 1+y^*+x^*-\lambda \end{vmatrix} = 0. \tag{3}$$

After solving this determinant, we get the eigenvalues $\lambda_\pm$. An equilibrium point is stable if $\lambda_\pm < 0$ otherwise unstable. The stability analysis of these three equilibrium points is studied in ref.[24].

(ii) Predator-Prey Model Map

Predator-Prey model map represented by the following system of difference equations [26,27]

$$x_{n+1} = ax_n(1 - x_n) - x_n y_n = f(x_n, y_n) \ , \tag{4}$$
$$y_{n+1} = bx_n y_n = g(x_n, y_n). \tag{5}$$

This model is used to understand the mechanism of competition between population of two species. Where x denotes the number of prey and y denotes the number of predator and a, b are the positive constant parameters, $(a, b > 0)$. Khan et al. [26] studied the local dynamics and bifurcations of a two dimensional discrete-time predator-prey model. The Predator-Prey model map possesses three equilibrium points for a particular value of a and b, namely, $(i)E_0 = (x^*, y^*) = (0, 0)$ for all parametric values of a and b, $(ii)E_1 = (x^*, y^*) = ((a - 1)/a, 0)$ for $a > 1$ and $(iii)E_2 = (x^*, y^*) = (1/b, (ab - a - b)/b)$ if $a > b/(b - 1)$ and $b > 1$. The stability determining eigenvalues are obtained from the following determinant,

$$\det(M - \lambda I) = \begin{vmatrix} a(1 - 2x^*) - y^* - \lambda & -x^* \\ by^* & bx^* - \lambda \end{vmatrix} = 0. \tag{6}$$

After solving this determinant, we get the eigenvalues $\lambda_\pm$. An equilibrium point is stable if $\lambda_\pm < 0$ otherwise unstable. The stability analysis of these three equilibrium points is studied in ref.[26]. Motivated by the above considerations, we wish to analyze the occurrence of VR and hysteresis phenomena in two maps. For this we need to drive them by the following biharmonic signal

$$F(n) = f \cos \omega n + g \cos \Omega n, \quad \Omega >> \omega \tag{7}$$

where $F(n)$ is added to the right hand side of Eqs.1 and 4. $f \cos \omega n$ and $g \cos \Omega n$ are the low- and high-frequency signals with the amplitudes f and g and ω and Ω are the frequencies of the low- and high- frequency signals.

3 Vibrational Resonance and Hysteresis in the Burgers Map

The difference equations of Burgers map with biharmonic signal is given by

$$x_{n+1} = (1 - \nu)x_n - y_n^2 + F(n) \ , \tag{8}$$
$$y_{n+1} = (1 + \mu)y_n + x_n y_n \ , \tag{9}$$

where subscript n represents iteration steps corresponding to the discrete-time evolution of the map. First, we analyze the occurrence of VR in the Burgers map (Eqs.(8-9)) for a particular parameters values of μ and ν. We fix $a = 0.15, b = 0.15$ and $\omega = 0.1$ and treat the amplitude g as the control parameter. We iterate the map with an initial value x_0 and leave the first 10^4 iterations as a transient. The solution of the map essentially contains a slow motion with the frequency ω and a fast motion with the frequency Ω. The amplitude

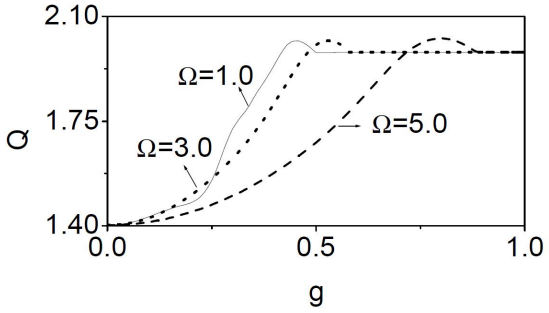

Fig. 1. Response amplitude Q versus g for three values of Ω, namely, $\Omega = 1, 3, 5$. The other parameters values are $\nu = 0.5, \mu = 0.1, \omega = 0.1$ and $f = 0.1$.

at the frequency ω increases and then decreases as g is varied, which is an indication of the occurrence of VR: the low-frequency ω is enhanced by the high-frequency signal. To quantify the occurrence of VR, we use the response amplitude Q of the Burgers map (Eqs.(8-9)) at the signal frequency ω. We focus our analysis on the low-frequency component of the output signal which exhibits resonance. From the numerical solution of x_n, the response amplitude Q is computed through $Q = \sqrt{Q_s^2 + Q_c^2}/f$, at the signal frequency, where

$$Q_s = \frac{2}{NT} \sum_{n=1}^{NT} x_n \sin\omega n, \tag{10}$$

$$Q_c = \frac{2}{NT} \sum_{n=1}^{NT} x_n \cos\omega n, \tag{11}$$

where $T = 2\pi/\omega$ and N is very large. In our numerical calculation of Q, N is chosen as 10^3. We analyze the response amplitude Q using the Eqs.(10-11) with $\nu = 0.5$ and $\mu = 0.1$ in the Burger's map for different values of low-frequency amplitude f and frequency (Ω) of the high-frequency signal. When g is varied, the response amplitude (Ω) increases to a maximum and then decreases resulting in the formation of peak and hence this phenomenon is termed as *vibrational resonance (VR)*. In Figure 1, $Q(\omega)$ is plotted for different values of Ω, namely, $\Omega = 1.0, 3.0$ and 5.0 with $\omega = 0.1$ and $f = 0.1$. For all values of Ω, single resonance is observed with the same response amplitude Q but the position of the peaks are shifted towards higher values of g with increasing Ω values. For $\Omega = 1.0, 3.0$ and 5.0 the maximum response amplitudes Q are observed at $g = 0.453, 0.5$ and 0.75 which is clearly shown in Figure 1. The non-resonant region is found to decrease with increase in Ω which is clearly evident in Figure 1.

Similarly we analyze the resonance pattern for $\nu = 0.5, \mu = 0.1, \omega = 0.1, \Omega = 1.0$ for three values of f, namely, $f = 0.05, 0.1, 0.15$ which is presented in Figure 2. For all values of f, single resonance is observed with the same response amplitude Q but the position of the maximum response amplitudes Q_{max} are shifted towards the lower values of g. That is, for $f = 0.05, 0.1, 0.15$,

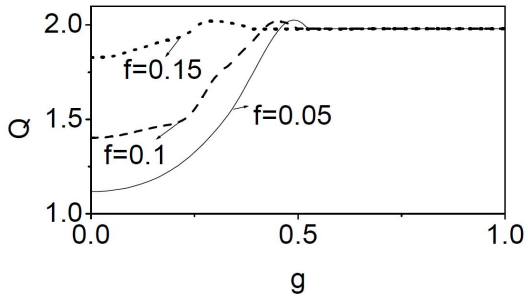

Fig. 2. Response amplitude Q versus g for three values of f, namely, $f = 0.05, 0.1, 0.15$ with $\nu = 0.5$ and $\mu = 0.1$. The other parameters values are $\omega = 0.1$ and $\Omega = 1.0$.

the maximum of the response amplitudes Q_{max} occur at $g = 0.255, 0.453, 0.5$ which is clearly evident in Figure 2. The non-resonant region is found to increase with increase in f which is clearly evident in Figure 2.

We describe the response curve in Figure 1. Figure 3 illustrates the nature of x_n for four values of g while $\nu = 0.5, \mu = 0.1, \omega = 0.1, \Omega = 1.0$ and $f = 0.1$. For $g = 0.0$ (that is, the map is driven by low-frequency signal $f \cos \omega n$ only) in Figure 3(a), a rapid switching between the equilibrium points occur. When the high-frequency signal $g \cos \Omega n$ is switched on, the oscillatory solutions of the map occur which is shown in Figures 3(b),3(c) and 3(d). However, as g increases, the modulation of x_n by the high-frequency signal $g \cos \Omega n$ and the shape of the trajectory profile changes from a sinusoidal to amplitude modulated sinusoidal pattern. This is clearly seen in Figure 3(b-d). The time duration between two consecutive returns to the neighbourhood of the fixed point is $\approx T(= 2\pi/\omega)$. The time duration decreases with a further increase in g.

The unperturbed Burgers map ($f = 0, g = 0$) exhibits complex dynamics, bifurcations like flip, pitchfork and Neimark-Sacker bifurcations and chaos for certain range of μ values with the fixed values of ν, which is presented in Figure 4. The bifurcation scenario of the Burgers map without biharmonic signal, when we vary the parameter μ with $\nu = 0.5, 1.0$ and 2.0 is shown in Figure 4. In Figures 4(a-c), it can be observed that there are more large invariant closed curves with a great abundance of periodic windows, which are from a Hopf bifurcation at $\mu = 0.4925$ and from regions of invariant closed curves to transient chaos along with complex periodic windows and chaos. For clarity, local amplifications of Figure 4(b) is shown in Figure 4(d). From this figure, we can clearly noticed the symmetry breaking of periodic orbits, interlocking period-doubling bifurcations and many complex windows in the chaotic regions. We have shown the occurrence of flip bifurcation in Figure 4(c). The phase portraits for various values of μ and ν in Figure 4(a) and Figure 4(b) are shown in Figure 5. From this diagram, one can clearly see that the interleaving occurrence of invariant closed curves and periodic orbits, Neimark-Sacker bifurcations and chaotic sets.

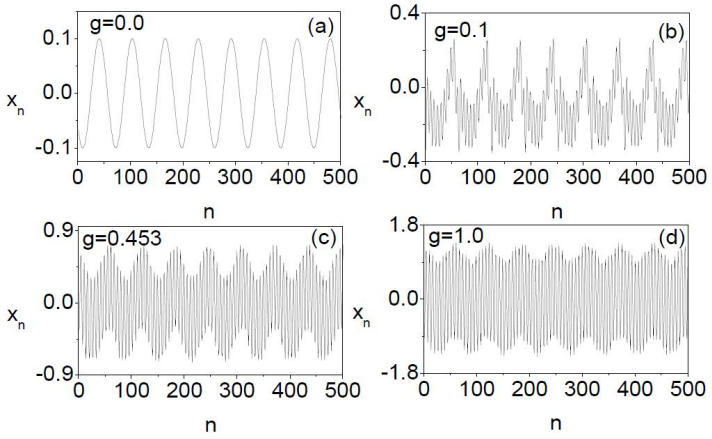

Fig. 3. Trajectory plot of x_n versus n for four values of g with $\nu = 0.5$ and $\mu = 0.1$. The other parameters values are $\omega = 0.1, \Omega = 1.0$ and $f = 0.1$.

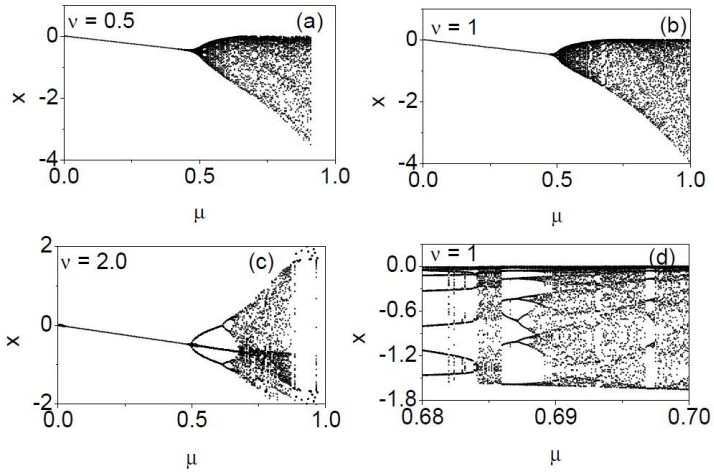

Fig. 4. Bifurcation diagram of the unperturbed Burgers map with (a) $\nu = 0.5$, (b) $\nu = 1.0$ and (c) $\nu = 2.0$. (d) Magnification of a part of Figure 4(b)

A large class of nonlinear dynamical systems is characterized by the coexistence of multiple attractors. It gives rise to the possibility of hysteresis, that is, the possibility of jumps through the coexisting attractors in a way that is not reversible when we fix a parameter back to its original value. Hysteresis is a typical phenomenon and is encountered in many scientific fields including magnetism, super conductivity and population dynamics. It exhibits both in discrete-time and continuous-time dynamical systems. Bifurcation diagram plotted by varying g in the forward direction as well as in the reverse direction is shown in Figure 6. Hysteresis behaviour is observed when g is varied.

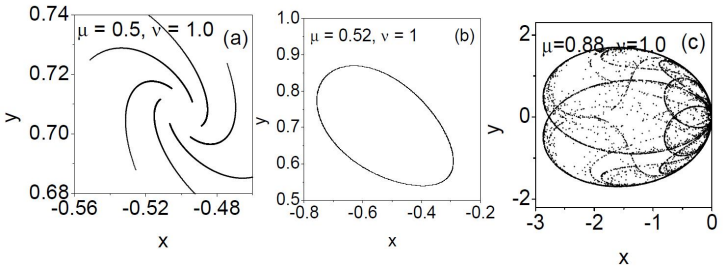

Fig. 5. Phase portraits of unperturbed Burgers map for some values of μ with $\nu = 1.0$
.

Figure 6(a) is obtained by varying the amplitude g from a small value in the forward direction. Figure 6(b) is obtained by varying g in the reverse direction from the value 1. Different paths are followed in the parameter g is varied smoothly from a small value to a larger and then back to a small value.

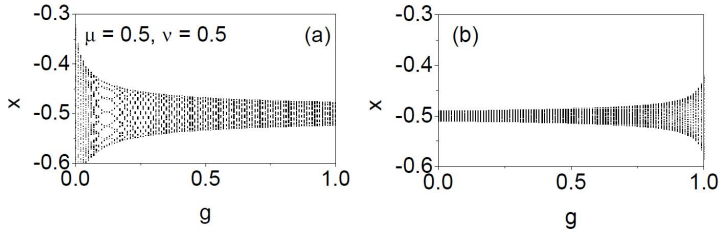

Fig. 6. Bifurcation diagrams (a) g is varied in the forward direction from 0. (b) g is varied in the reverse direction from 1.0. The parameters values are fixed as $\mu = 0.5, \nu = 0.5, f = 0.1, \omega = 0.1$ and $\Omega = 5.0$
.

4 Vibrational Resonance and Hysteresis in the Predator-Prey Map

In the previous section, we studied the occurrence of VR and hysteresis in the Burgers map. In this section, we analyze the occurrence of VR and hysteresis phenomena in the Predator-Prey map. The difference equations of the Predator-Prey map driven by biharmonic signal is given by

$$x_{n+1} = ax_n(1 - x_n) - x_n y_n + F(n)\ , \tag{12}$$

$$y_{n+1} = bx_n y_n. \tag{13}$$

where n represents iteration steps corresponding to the discrete-time evolution of the map. Hysteresis and jump behaviours are not observed in this map.

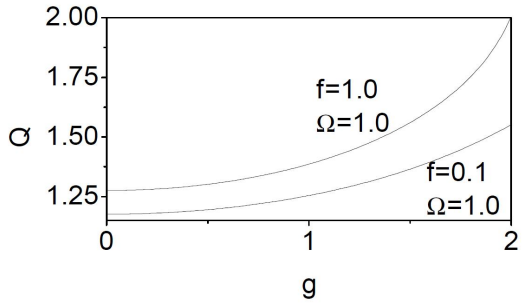

Fig. 7. Response amplitude Q versus g for the frequency ratio $\frac{\Omega}{\omega} = 10$ with $a = 0.15, b = 0.15, \omega = 0.1$ and $f = 0.1, 1.0$

.

We numerically analyze the occurrence of VR for the parameters values of a and b and treat the amplitude g of the high-frequency signal as the control parameter. We analyze the effect of biharmonic signal for three frequency ratios, namely, $\frac{\Omega}{\omega} = 10$ (that is $\omega = 1.0$ and $\Omega = 10$), $\frac{\Omega}{\omega} = 50$ (that is $\omega = 1.0$ and $\Omega = 50$) and $\frac{\Omega}{\omega} = 60$ (that is $\omega = 1.0$ and $\Omega = 60$). For these three frequency ratios, the evolution of the response amplitude Q versus the high-frequency signal amplitude g are shown in Figure 7 and Figure 8 for $a = 0.15$ and $b = 0.15$. In Figure 7, for the frequency ratio $\frac{\Omega}{\omega} = 10$, Q increases with g but no resonance occurs for $f = 0.1$ and $f = 1.0$ which is clearly shown in Figure 7.

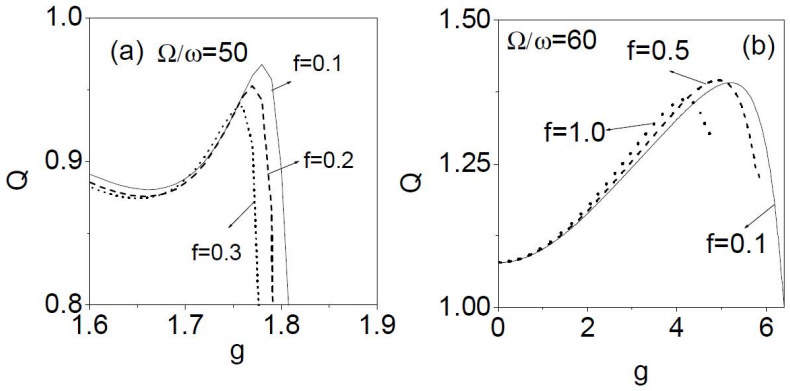

Fig. 8. Response amplitude Q versus g for the frequency ratios (a) $\frac{\Omega}{\omega} = 50$ and (b) $\frac{\Omega}{\omega} = 60$ with $a = 0.15, b = 0.15, \omega = 0.1$ and $f = 0.1, 0, 2, 0.3$

.

Next we study the occurrence of VR for the frequency ratios $\frac{\Omega}{\omega} = 50$ and $\frac{\Omega}{\omega} = 60$. The corresponding numerical results are shown in Figure 8(a) and

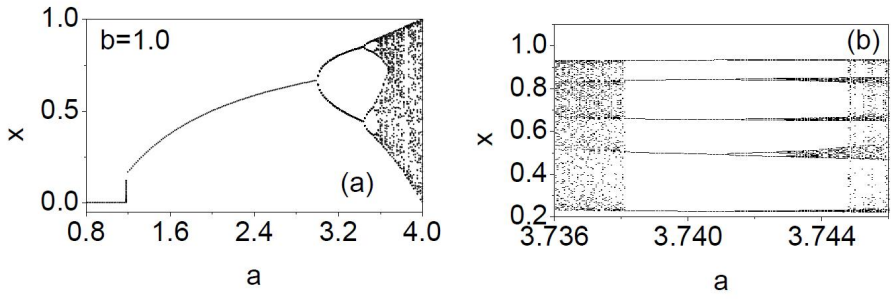

Fig. 9. Bifurcation diagram of the unperturbed predator-prey map with $b = 1.0$ (b) Magnification of a part of Figure 9(a)

Figure 8(b). Figure 8(a) shows the variation of numerically computed Q against the control parameter g for the frequency ratio $\frac{\Omega}{\omega} = 50$. with $a = 0.15, b = 0.15$ and $f = 0.1, 0.2, 0.3$. For all values of f, single resonance is observed which is clearly shown in Figure 8(a). The first striking effect is that the maximum of the resonance curve diminishes as f increases and at the same time, its location shifted towards lower values of the high-frequency signal amplitude g. No resonance is observed when $g < 1.65$ and $g > 1.8$ for all values of f. Then we analyze the occurrence of VR for another frequency ratio $\frac{\Omega}{\omega} = 60$ which is presented in Figure 8(b). For this frequency ratio we observed a single resonance for all values of f and the position of the peak shifted towards lower values of the high-frequency signal amplitude g.

The unperturbed Predator-prey model ($f = 0, g = 0$) exhibits new and interesting dynamical behaviours such as Neimark-Sacker and period-doubling bifurcations, a stable invariant closed curve and chaos for certain range of a values with the fixed value of b. For example, the bifurcation pattern for the predator-prey map described by the Eqs.(4-5) is shown in Figure 9(a). The local dynamics of the map is clearly seen in Figure 9(b) which is the magnification of a part of Figure 9(a). At the critical value of the control parameter a, the stability of equilibrium points is exchanged or transformed. This type of bifurcation is called transcritical bifurcation. At $a = a_c = 1.2$, a transcritical bifurcation occurs at which maximal Lyapunov exponent ($\lambda \approx 0$). When a is further increased from $a = 1.2$, the system undergoes both a Neimark-Sacker bifurcation and a period-doubling bifurcation. Onset of chaos is observed at $a = 3.6$. For $3.6 < a < 4.0$, a chaotic motion is found. It shows that periodic motion and chaotic motion for the range $a \in [1.2, 4.0]$. When the parameter a is increased beyond the onset of chaos, the dynamics of the system is not fully chaotic alone but many changes in the dynamics takes place at different critical values of a. Particularly, the chaotic orbits interspersed by periodic windows, intermittent chaos, period-doubling bifurcation and bifurcations of chaos which include band-merging, sudden-widening, sudden destruction crises, which are clearly evident in Figure 9(b). Due to the effect of biharmonic signal perturbation, hysteresis phenomenon is not observed in the predator-

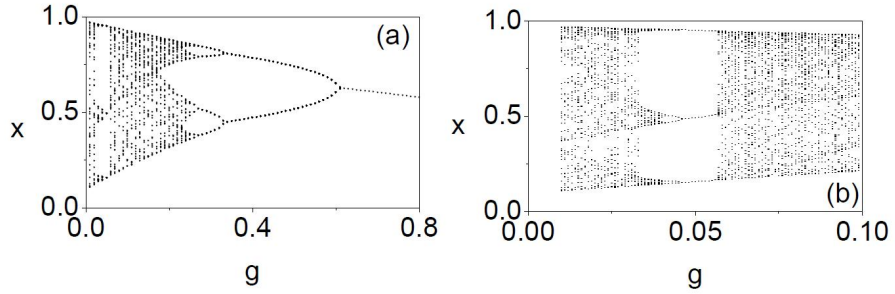

Fig. 10. Bifurcation diagram of the perturbed predator-prey map with $a = 3.5$ and $b = 1.0$ (b) Magnification of a part of Figure 10(a) The parameters values are fixed as $\omega = 0.1, \Omega = 5.0$ and $f = 0.1$
.

prey model (Eqs.(12-13)). But the coexistence of several attractors, reverse period-doubling bifurcation, periodic windows and chaotic orbits are observed when the control parameter g is varied. The bifurcation pattern for the system described by Eqs.(12-13) is shown in Figure 10(a) and Figure 10(b) gives the magnification of a part of Figure 10(a). The local dynamics of the map (Eqs.(12-13)) is clearly seen in Figure 10(b). We fix the other parameters values as $a = 3.5, b = 1.0, f = 0.1, \omega = 0.1$ and $\Omega = 5.0$. From Figure 10(a), it is clearly depicted that with the inclusion of biharmonic signals the map (Eqs.(12-13)) follows reverse period-doubling route to chaos instead of period-doubling route to chaos. More importantly, these period-doubling reversals may be used to control chaos, as they have the potential to suppress dangerous chaotic fluctuations. The period doubling reversals phenomenon occurs in models of insect population [28,29], annual plant populations [30], host-parasitoid interactions [31] and systems of competing species [32]. The presence of reversals has also been documented in other areas of research, ranging from models of magnetoconvection [33] and rotating galaxies [34], to a neuronal model of psychotic human behaviour [35].

5 Conclusion

In the present work, we numerically studied the occurrence of vibrational resonance in two particular two-dimensional maps like Burgers map and Predator-Prey map under the influence of biharmonic signal. Here we have shown that the low- frequency signal greatly enhanced by the high-frequency signal in a resonant way. From the numerical analysis, we observed single resonance peak for a specific set of values of the parameters of the maps such as amplitude g and frequency Ω of the high-frequency signal. Apart from the VR phenomenon, hysteresis behaviour is encountered in Burgers map. We have observed variety of complex behaviours such as reversal of period-doubling bifurcations, periodic and chaotic sets for a certain range of parameters values of the maps. We

further verified our findings with the help of bifurcation diagram, phase portrait and response amplitude Q. Investigation of other types of resonances such as stochastic resonance, parametric resonance, ghost-vibrational resonance and coherence resonance in these maps may provide interesting results. These will be studied in future.

References

1. P.S. Landa and P.V.E. McClintock, Vibrational Resonance, *J.Phys. Math. Gen.*, vol.33: L433-L438, 2000.
2. S. Jeyakumari, V. Chinnathambi, S. Rajasekar and M.A.F. Sanjuan, Single and Multiple Vibrational Resonance in a Quintic Oscillator in the Monostable Potentials, *Physical Review E*, vol.80: 046608, 2009.
3. M. Gitterman, A Bistable Oscillator Driven by Two Periodic Fields, *J. Phys. A*, vol.34: L355-L357, 2001.
4. J.P. Baltanas, L. Lopez, I. Blechman, P.S. Landa, A. Zaikin and J. Kurths, Experimental Evidence, Numerics, and Theory of Vibrational Resonance in Bistable Systems, *Phys. Rev. E*, vol.67: 066119, 2003.
5. I.I. Blckhman and P.S. Landa, Conjugate Resonances and Bifurcations in Nonlinear Systems Under Biharmonical Excitation, *Int. J. Non-Linear Mech.*, vol.39: 421-426, 2004.
6. S. Rajasekar, K. Abirami and M.A.F. Sanjuan, Novel Vibrational Resonance in Multistable Systems, *Chaos*, vol.21: 033106, 2011.
7. S. Jeyakumari, V. Chinnathambi, S. Rajasekar and M.A.F. Sanjuan, Vibrational Resonance in a Quintic Oscillator, *Chaos*, vol.19: 043128, 2009.
8. V.N. Chizhevsky, and G. Giacomelli, Experimental and Theoretical Study of Vibrational Resonance in a Bistable System with Asymmetry, *Phys. Rev. E*, vol.73: 022103, 2006.
9. J.H. Yang and X.B. Liu, Delay Induces Quasi-periodic Vibrational Reosnance, *J. Phys. A: Math. Theor.*, vol.43: 122001, 2010 .
10. C. Jeevarathinam, S. Rajasekar and M.A.F. Sanjuan, Theory and Numerics of Vibrational Resonance in Duffing Oscillator with Time Delayed Feedback, *Physical Review E*, vol.83: 066205, 2011.
11. A. DazaAlvar, D. Wagemakers, S. Rajasekar and M.A.F. Sanju Vibrational Resonance in a Time-Delayed Genetic Toggle Switch, *Communications in Nonlinear Science and Numerical Simulation*, vol.18(2): 411-416, 2013.
12. C. Jeevarathinam, S. Rajasekar and M.A.F. Sanjuan, Vibrational Resonance in Groundwater-Dependent Plant Ecosystems, *Ecological Complexity*, vol.15: 1-37, 2013.
13. C. Yao and M. Zhan, Signal Transmission by Vibrational Resonance in One-way Coupled Bistable Systems, *Phys. Rev. E*, vol.81: 061129, 2010.
14. V.M. Gandhimathi, S. Rajasekar and J. Kurths, Vibrational and Stochastic Resonances in Overdamped two Coupled Anharmonic Oscillators, *Phys. Lett. A*, vol.360: 279-286, 2006.
15. Paul Shibashis and Shankar Ray Deb, Vibrational resonance in a driven two-level quantum system, linear and nonlinear response, *Phil. Trans. R. Soc. A*, vol.379, 20200231 (2021) 1http://doi.org/10.1098/rsta.2020.023.
16. A. Chowdhury, M.G. Clerc and S. Barbay, et al. Weak signal enhancement by nonlinear resonance control in a forced nano-electromechanical resonator, *Nat Commun*, vol. 11, 2400 (2020). https://doi.org/10.1038/s41467-020-15827-3.

17. A. Jeevarekha, M. Santhiah and P. Philominathan, Enriched Vibrational in Certain Discrete System, *Pramana J of Phys.*, vol.83(4): 493-504, 2014.
18. S. Rajasekar, J. Used, A. Wagemakers and M.A.F. Sanju Vibrational Resonance in Biological Nonlinaer Maps, *Communications in Nonlinear Science and Numerical Simulation*, vol.17: 3435-3445, 2012.
19. V.N. Chizhevsky and G. Giacomelli, Vibrational Resonance and Detection of Aperiodic Binary Signal, *Phys. Rev. E*, vol.77: 051126, 2008.
20. V.N. Chizhevsky, Analytical Study of VR in an Overdamped Bistable Oscillator, *Int. J. of Bifur. & Chaos*, vol.18: 1767-1774, 2008.
21. R. Jothimurugan, K. Tamilmaran, S. Rajasekar and M.A.F. Sanju Experimental Evidence for VR and Enhanced Transmission in Chua's Cirucuit, arXiv: 1308.2463v1 [nlin.CD] 12 Aug 2011.
22. K. Abirami, S. Rajasekar and M.A.F. Sanjuan, Vibrational and Ghost Vibrational Resonance in a Modified Chua's Circuit Model Equation, *Int.J.Bifur.Chaos*, vol.24: 1430031, 2014.
23. J.M. Burgers, Mathematical Examples Illustrating Relations occurring in the Theory of Turbulent Fluid Motion, *Trans. Roy. Acad. Sci. Amsterdam*, vol.17: 1-53, 1939
24. EM. ELabbasy, H.N. Agiza, H.EL.Metwally and A.A. Elsadany, Bifurcation Analysis, Chaos, and Control in the Burgers Mapping, *Int. J. of Nonlinear Science*, vol.4: 171-185, 2007.
25. R. Senkerik, I. Zelinka, M. Pluhacek and Z.K. Oplatkova, Evolutionary Control of Chaotic Burgers Map by means of Chaos Enhanced Differential Evolution, *International Journal of Mathematics and Computers in Simulation*, vol.8: 39-45, 2014.
26. Abdul Qadeer Khan, Bifurcations of a Two-dimesional Discrete-Time Predator-Prey model, Advances in Differential Equations, vol.56: 1-33, 2019.
27. M. Danca, S. Codreanu and B. Bak, Detailed Analysis of a Nonlinear Prey-Predator Model, *Journal of Biological Physics*, vol.23: 1120, 1997.
28. T.S. Jr Bellows, The descriptive properties of some models for density dependence, *J. Anim. Ecol.*, vol.50: 139-156, 1981.
29. M.P. Hassell, J.H. Lawton and R.M. May, Patterns of dynamical behaviour in single-species populations, *J. Anim. Ecol*, vol.45: 471-486, 1976.
30. S.W. Pacala and J.A. Silander, Neighborhood Models of Plant Population Dynamics, I. Single-Species Models of Annuals, *Am. Nat.*, vol.125: 385-411, 1985.
31. R.M. May, Regulation of Populations with Nonoverlapping Generations By Microparasites: A Purely Chaotic System, *Am. Nat.*, vol.125(4): 573-584, 1985.
32. R.M. May, Biological population with non-overlapping generations: stable point, stable cycle and chaos, *Science*, vol.186: 645-647, 1974.
33. E. Knobloch and N.O. Weiss, Bifurcations in a model of magnetoconvection, *Physica*, vol.9D: 379-407, 1983.
34. G. Contopoulos, Inverse Feigenbaum sequences in Hamiltonian systems, *Lett. Nuovo Cimento*, vol.37: 149-153, 1983.
35. R. King, J.D. Barchas and B.A. Huberman, Chaotic Behavior in Dopamine Neurodynamics, *Proc.Natn. Acad. Sci. U.S.A.*, vol.81: 1244-1247, 1984.